



Kahramanmaraş Sütçü İmam University

Journal of Engineering Sciences



Geliş Tarihi : 25.01.2025
Kabul Tarihi : 22.03.2025

Received Date : 25.01.2025
Accepted Date : 22.03.2025

LUMINANCE ESTIMATION FROM SURFACES WITH DIFFERENT COLOR TEMPERATURE AND LAMP ILLUMINATION ANGLE: A DEEP LEARNING-BASED APPROACH

FARKLI RENK SICAKLIĞI VE AYDINLATMA AÇISI İLE YÜZEYLERDEN PARILTI TAHMİNİ: DERİN ÖĞRENME TABANLI BİR YAKLAŞIM

Birkan BÜYÜKARIKAN^{1*} (ORCID: 0000-0002-9703-9678)
Erkan ÜLKER² (ORCID: 0000-0003-4393-9870)

¹ Isparta Uygulamalı Bilimler Üniversitesi, Uluborlu Selahattin Karasoy Meslek Yüksekokulu, Bilgisayar Teknolojileri, Isparta, Türkiye
² Konya Teknik Üniversitesi, Mühendislik ve Doğa Bilimleri Fakültesi, Bilgisayar Mühendisliği, Konya, Türkiye

*Sorumlu Yazar / Corresponding Author: Birkan BÜYÜKARIKAN, birkanbuyukarikan@isparta.edu.tr

ABSTRACT

Traditional methods of luminance estimation are performed with the help of electronic systems. However, the changes in lighting properties, such as color temperature and the lamp illumination angle, affect the luminance on the object, making luminance estimation difficult compared to traditional methods. Therefore, this study proposes an image-based approach using convolutional neural networks (CNNs) models to provide an alternative solution for luminance estimation. In this study, luminance estimation is performed on defective and healthy apple images by considering the effects of color temperature and lamp illumination angle. According to the results, the GoogLeNet model exhibited the best performance at values where the learning rate was 0.001 and the batch size was eight. It also performed the best luminance estimation with a lower Root Mean Square Error (RMSE) value. According to color temperatures, defective apples showed the lowest RMSE value at warm white light, and healthy apples showed the lowest RMSE value at cold white light. According to color temperatures, the best luminance estimation is a 5.023 cd/m² RMSE value at a cold white light. According to lamp angle, defective apples obtained the lowest RMSE value at 5.106 cd/m² at a 60-degree angle, and healthy apples obtained the lowest RMSE value at 6.411 cd/m² at a 45-degree angle.

Keywords: Luminance estimation, color temperature, lamp illumination angle, deep learning

ÖZET

Geleneksel yöntemlerle parıltı tahmini, elektronik sistemler yardımıyla gerçekleştirilmektedir. Ancak, nesne üzerindeki parıltıyı etkileyen renk sıcaklığı ve lambanın nesneyi aydınlatma açısı gibi aydınlatma özelliklerinin değişimi geleneksel yöntemlerle parıltı tahminini zorlaştırmaktadır. Dolayısıyla bu çalışmada, parıltı tahminine alternatif bir çözüm sunmak amacıyla evrimsel sinir ağları (CNN) modellerinden yararlanılarak görüntü tabanlı bir yaklaşım önerilmiştir. Çalışmada, renk sıcaklığı ve lambanın konum açısının etkileri göz önünde bulundurularak, kusurlu ve kusursuz elma görüntüleri üzerinde parıltı tahmini yapılmıştır. Elde edilen sonuçlara göre, GoogLeNet modeli, öğrenme oranının 0.001 ve yığın boyutunun 8 olduğu değerlerde en iyi performansı sergileyerek, daha düşük Karekök Ortalama Kare Hata (RMSE) değeri ile en iyi parıltı tahminini gerçekleştirmiştir. Renk sıcaklıklarına göre, kusurlu elmalar en düşük RMSE değerini 2700 K renk sıcaklığında ve kusursuz elmalar ise en düşük RMSE değerini 6500 K renk sıcaklığında göstermiştir. Renk sıcaklıklarına göre; en iyi parıltı tahmini, 6500 K renk sıcaklığında 5.023 cd/m² RMSE değerindedir. Lamba açısına göre; kusurlu elmalar en düşük RMSE değerini 60 derecelik açıda 5.106 cd/m² ve kusursuz elmalar en düşük RMSE değeri ise 45 derecelik açıda 6.411 cd/m² olarak elde etmiştir.

Anahtar Kelimeler: Parıltı tahmini, renk sıcaklığı, lambanın aydınlatma açısı, derin öğrenme

INTRODUCTION

Color temperature, as one of the important properties of light, is widely used in image analysis and visual comfort-related applications (Luo, 2011; Holtzschue, 2012). In image analysis, the color temperature feature significantly impacts color accuracy and overall image quality. Light from a white light source with different color temperatures changes the brightness, color tones, and contrast, thereby changing the details and clarity of the perceived image (Wu et al., 2010; Luo, 2011; Holtzschue, 2012; Hong et al., 2017).

The color temperature (CCT) of the light source, measured in Kelvin (K) value, defines the whiteness of a light (Sims et al., 2021). This value helps us to understand the temperature of the color of the light. Lower color temperatures represent warmer colors (reddish), and higher color temperatures represent cooler colors (bluish). So, in the real world, white light sources do not always provide the same white light characteristics (Holtzschue, 2012; Sharma and Bala, 2017). Therefore, the color temperatures of light sources used in machine vision applications are important for the accurate and consistent perception of colors in images. Also, color temperature is critically important in evaluating the performance of light sources (Huang et al., 2017; Huang and Wei, 2021).

In machine vision applications, the angle at which the lamp illuminates the object is another important parameter related to image analysis and visual comfort. This angle has a significant effect on the perception of the surface texture of an object and the clarity of the detail captured by vision systems. Light from low angles creates more shadows on the object's surface, allowing texture information to be displayed more clearly. In contrast, light from high angles provides a more even illumination, helping to accurately perceive colors and tones on the surface (Manav, 2005; Benweilght, 2021).

As a result, the effects of color temperature and lamp angles on images are important research topics in image processing. In particular, the relationship between color temperature and lamp illumination angle and luminance can not only help analyze images more accurately (Luo, 2011; Holtzschue, 2012; Catalbas and Kobav, 2022; Kamath et al., 2022) but also provide benefits in areas such as object recognition (Nie and Lv, 2023), industrial process control (Odabas et al., 2023), and medical imaging (Wang et al., 2024). These approaches will also open new horizons in extracting more information from visual data and transforming this information into applications.

In recent studies, deep learning-based models such as convolutional neural networks (CNNs) have been effectively used for luminance estimation. The interaction between luminance, color temperature, and lamp illumination angle significantly affects surfaces' perceived brightness and color accuracy. CNNs can make more precise estimations by learning the relationships between these complex visual features (Kim et al., 2018; Liu et al., 2020b). The ability of CNNs to accurately predict their transmissions offers inferences applicable in various environments, from outdoors to indoors. For example, Kayakuş and Çevik (2019) estimated the luminance in road lighting with a deep neural network (DNN) model they developed using the R, G, and B pixel values of road images. Similarly, Simon and Uma (2022) used features extracted from deep architectures and luminance values of images to effectively classify texture images and classified these features with SVM. Yang et al. (2021) obtained images of different scenes under different azimuthal angles and color temperatures (e.g., 2500 K and 4500 K) and calibrated the illumination settings of these images according to the input image and corresponding depth maps using the Multi-Mode Forked Network (MB-Net) model they proposed. On the other hand, Songwa et al. (2021) used images to estimate the luminance on office desks and created a CNN model based on the Y parameter. This study highlights the effectiveness of image-based luminance estimation. The above studies demonstrate the importance of luminance estimation in direct applications and in the development of more robust and versatile CNN models. As researchers continue to innovate and improve their approaches, more robust solutions for luminance estimation can be produced by integrating versatile techniques. Furthermore, developing these approaches will better understand the complex interactions between light conditions and visual perception, providing more effective solutions for real-world applications. This is the primary motivation for this study.

This study aims to develop a CNN-based approach for luminance estimation from images. In this study, an original dataset containing different color temperatures (2700, 4000, and 6500 K), lamp illumination angles (30, 45, and 60 degrees), object position angles (0, 90, 180, and 270 degrees) and object-to-camera distance (30, 35, and 40 cm) was created. Apples with and without defects were used as objects, and images of apples were obtained through a closed system. GoogLeNet and Xception models were used for luminance estimation and evaluated according to the Y parameter received from the images. In addition, models were run with different hyperparameters. Models were

evaluated according to different color temperatures and lamp angles with a 3-fold cross-validation method. This study was examined using mean square error (MSE), mean absolute error (MAE), root mean square error (RMSE), and mean absolute percentage error (MAPE) criteria. The contributions of this study to the literature are summarized below:

- In this study, an original dataset includes different color temperatures, lamp illumination angles, object position angles, and image acquisition distances. This dataset will provide an important resource for research on luminance estimation.
- The images used for luminance estimation were obtained in a controlled, closed system. This ensures that the images are taken correctly and provides reliable data for luminance estimation by providing results verified by electrical and photometric measurements.
- In this study, luminance estimation was performed using deep learning-based GoogLeNet and Xception models, and the best performance of the models was achieved with different hyperparameters. These analyses were evaluated according to both color temperature and lamp illumination angle. The limited number of studies on this subject in literature increases the importance of research in guiding future studies.

MATERIAL AND METHODS

Experimental System and Lighting Sources

In machine vision applications, eliminating the effects of natural lighting conditions on the image is critical (Brosnan and Sun, 2004). Because color images are sensitive to ambient light conditions, they can affect the consistency in analytical processes and increase the margin of error in photometric measurements (Li et al., 2016; Ileri et al., 2019). To minimize this effect in studies, it is recommended to create a controlled imaging environment, in other words, to obtain images from a closed imaging cabin system (Girolami et al., 2013; Ma et al., 2017; Kandpal et al., 2019). Therefore, a closed cabin system was built to capture images in this study. Designed with dimensions of 60x60x80 cm³ (width, depth, and height), the cabin contains a camera, lens, elevator system, and lighting sources. The lighting sources in the system provide the opportunity to illuminate the object from different angles while also making it possible to move the object closer to the camera and further away. In addition, LED lamps providing white light were used to illuminate the objects in this study (Büyükarıkan, 2022).

During image acquisition, some areas of the cabin system may receive more light than others. This may affect the total amount of light reflected from the object, causing differences in the image's brightness level (Saldaña et al., 2013). To avoid this problem, two illumination sources were used in the cabin (Xu et al., 2022).

The light captured by a camera is affected by components such as spectral properties and the shape of the illumination (Smith, 2000; Aleixos et al., 2002; Unay and Gosselin, 2005). These components play an essential role in various parameters, such as the illumination quality and the image's appearance (Liu et al., 2020a). This study considered color temperature and illumination shape (the angle at which the lamp illuminates the object).

As seen in Table 1, white light sources are divided into three main groups according to their color temperatures. The first group is warm white light sources below 3300 K. These lights are perceived as having a reddish or yellowish tone. The second group, cool warm white lights in the 3300-5300 K range, offer a more natural white tone. The third group is cold white light sources above 5300 K. These lights have a bluish tone (Büyükarıkan, 2022). In this study, low CCT warm white (2700 K), medium CCT cool white (4000 K), and high CCT cold white (6500 K) LED lighting sources were used to provide white light.

Table 1. Relationship Between Color Temperature and Light Color (Kocabey, 2008; Özkaya and Tüfekçi, 2011).

CCT (K)	Light color temperature
<3300	Warm white light
3300-5300	Cool white light
>5300	Cold white light

Another lighting component used in this study, the lighting type, is an essential factor that changes the image quality by affecting the luminance in the image (Iacomussi et al., 2015; Shi and Chen, 2021). In machine vision applications, in frontal lighting, which is based on the forward transmission of light to obtain surface features, the lighting sources are placed in the same direction as the camera (Yang, 1994). In addition, in frontal lighting, the lamp's angle significantly affects the light distribution on the object. To observe these effects, the lighting sources were placed to

illuminate the object at 30°, 45°, and 60° angles (Büyükarıkan, 2022; Sumon, 2022). In this arrangement, all lighting sources were operated at a 100% brightness level (Büyükarıkan, 2022). Figure 1 shows the system structure from which the images were taken.

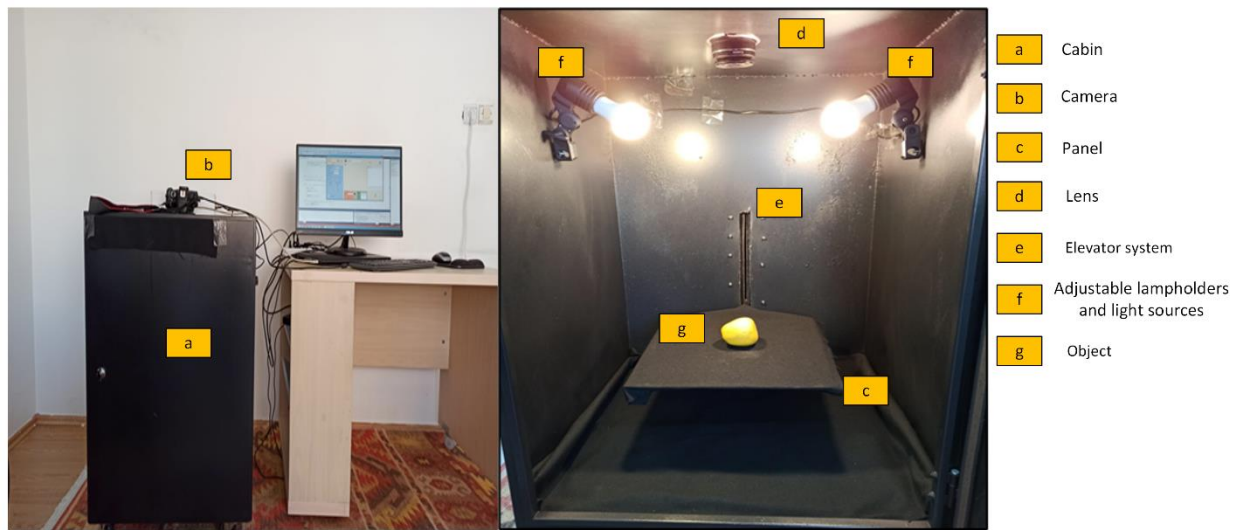


Figure 1. The Cabin Used for Image Acquisition (Büyükarıkan, 2022).

Dataset Details

In the literature, 2700 K white light, 6500 K white light (at different dimming levels), and green light have been used in studies on the classification of physiological disorders (bitter pit, shriveling, and superficial scald) in Golden Delicious and Granny Smith apple varieties (Buyukarikan and Ulker, 2022; 2023) and illumination estimation from images (Büyükarıkan and Ülker, 2022). In these studies, images were taken at 4 different position angles (0, 90, 180, and 270 degrees), at 2 object-to-camera distances (35 and 45 cm), and with a light intensity of 45 degrees on the apple. A total of 1080 images were taken. This study uses a lighting scenario based on the color temperature of different white lights and the angle of the lamp. The Golden Delicious apple variety was chosen as the object, and an original data set was created using defective (shriveling) and healthy apples. Images of each defective and healthy apple were taken under three different lighting conditions (warm white, cool white, and cold white), four different object positions (0, 90, 180, and 270 degrees), three object-to-camera distance (30, 35, and 40 cm) and three different lamp illumination angles (30, 45, and 60 degrees) and a total of 216 images were obtained. Then, the images were enriched with enhancement methods such as cropping, flipping, rotating, and shifting. A total of 1296 images were obtained with these methods, and these images were evaluated in terms of the defective conditions of the apples and recorded according to their color temperatures and lamp illumination angles. This dataset was produced in the author's previous study (Büyükarıkan, 2022).

In this study, images were recorded by varying two basic parameters, color temperature and lamp illumination angle. To isolate the effects of these parameters, all lamp illumination angles were used in the color temperature analysis, and all color temperatures were used in the lamp illumination angle analysis. Thus, the effects on luminance estimation were more clearly demonstrated. Also, there are equal numbers of images in both datasets created according to color temperatures and lamp angles. Thus, balanced classes were made in the dataset. Table 2 lists these details of the dataset.

Table 2. Details of the Datasets Used for Luminance Estimation.

Lamp sources		Defective apple (original)	Healthy apple (original)	Defective apple (enhancement)	Healthy apple (enhancement)	Total
Color temperature	Lamp angel					
Warm white	30	36	36	216	216	432
Cool white	45	36	36	216	216	432
Cold white	60	36	36	216	216	432
Total		108	108	648	648	1296

Some images obtained with different color temperatures, object positions, lamp illumination angles, and defect types are presented in Figure 2. The first row shows defective apples, and the second shows healthy apples. Also, the images in the first column were obtained at 2700 K (Fig. 2a and Fig. 2d), the second column at 4000 K (Figure 2b and Figure 2e), and the last column at 6500 K (Figure 2c and Figure 2f).

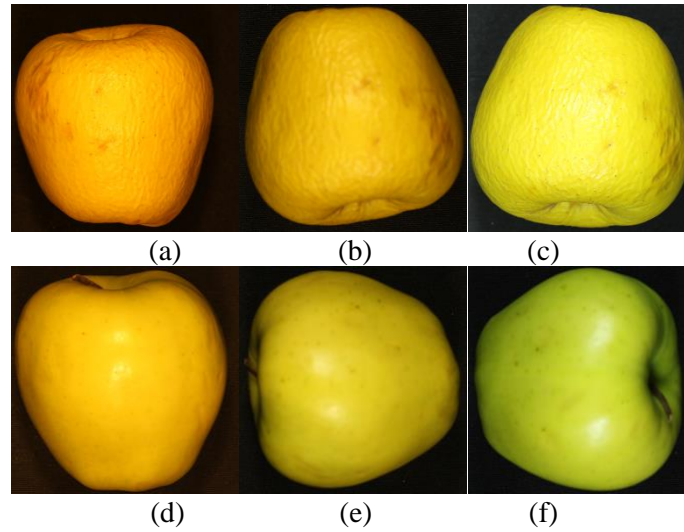


Figure 2. The Dataset (Büyükarıkan, 2022) **a.** Defective Apple in 30-Degree Lamp Angle and Warm White Light Type **b.** Defective Apple in 45-Degree Lamp Angle and Cool White Light Type **c.** Defective Apple in 60-Degree Lamp Angle and Cold White Light Type **d.** Healthy Apple in 45-Degree Lamp Angle and Warm White Light Type **e.** Healthy Apple in 30-Degree Lamp Angle and Cool White Light Type **f.** Healthy Apple in 60-Degree Lamp Angle and Cold White Light Type.

Deep Learning Models: GoogLeNet and Xception

Two well-known CNN models that are commonly favored in the deep learning space are GoogLeNet and Xception. In studies analyzing different lighting scenarios (Büyükarıkan and Ülker, 2022; Buyukarikan and Ulker, 2023), GoogLeNet and Xception models were reported to perform well in tasks such as image classification and illumination estimation from images. Based on these findings, these two models were considered for luminance estimation from apple surfaces (Büyükarıkan, 2022).

Chollet (2017) suggested Xception (Extreme Inception) as a more sophisticated iteration of the Inception architecture. The depthwise separable convolution notion, which is popular in deep learning, was first shown by this model. The Xception model's default input size is 299x299x3. GoogLeNet, on the other hand, is renowned for its Inception architecture and was created by Szegedy et al. (2014). This architecture provides a deep and computationally efficient structure. GoogLeNet's default input size is 224x224x3. GoogLeNet can perform well even on devices with fewer resources, however, Xception provides higher accuracy rates on systems with more processing power.

Proposed Approach

The change of white color depending on color temperatures and the lighting type's effect on the image's luminance causes the cameras to perceive images differently. In this study, an image-based approach for luminance estimation using CNN models is proposed from images obtained depending on the object's color temperature and the lamp illumination angles (Büyükarıkan, 2022). The details of the proposed approach are shown in Figure. 3.

A general equation is used for the luminance level. In this study, the luminance values of the images were first calculated by applying the inequality in Equation 1 (Songwa et al., 2021). These values constitute the output values of the CNN models. Then, the luminance was estimated from the images using CNN models. The estimation was performed on the images obtained according to the color temperature and the lamp's illumination angle on the object.

$$Y = R*0.2125 + G*0.7125 + B*0.0721 \quad (1)$$

This equation calculates the Y value of a pixel using the red (R), green (G), and blue (B) pixel values in the RGB color model. The Y value represents the luminance level of a colored pixel.

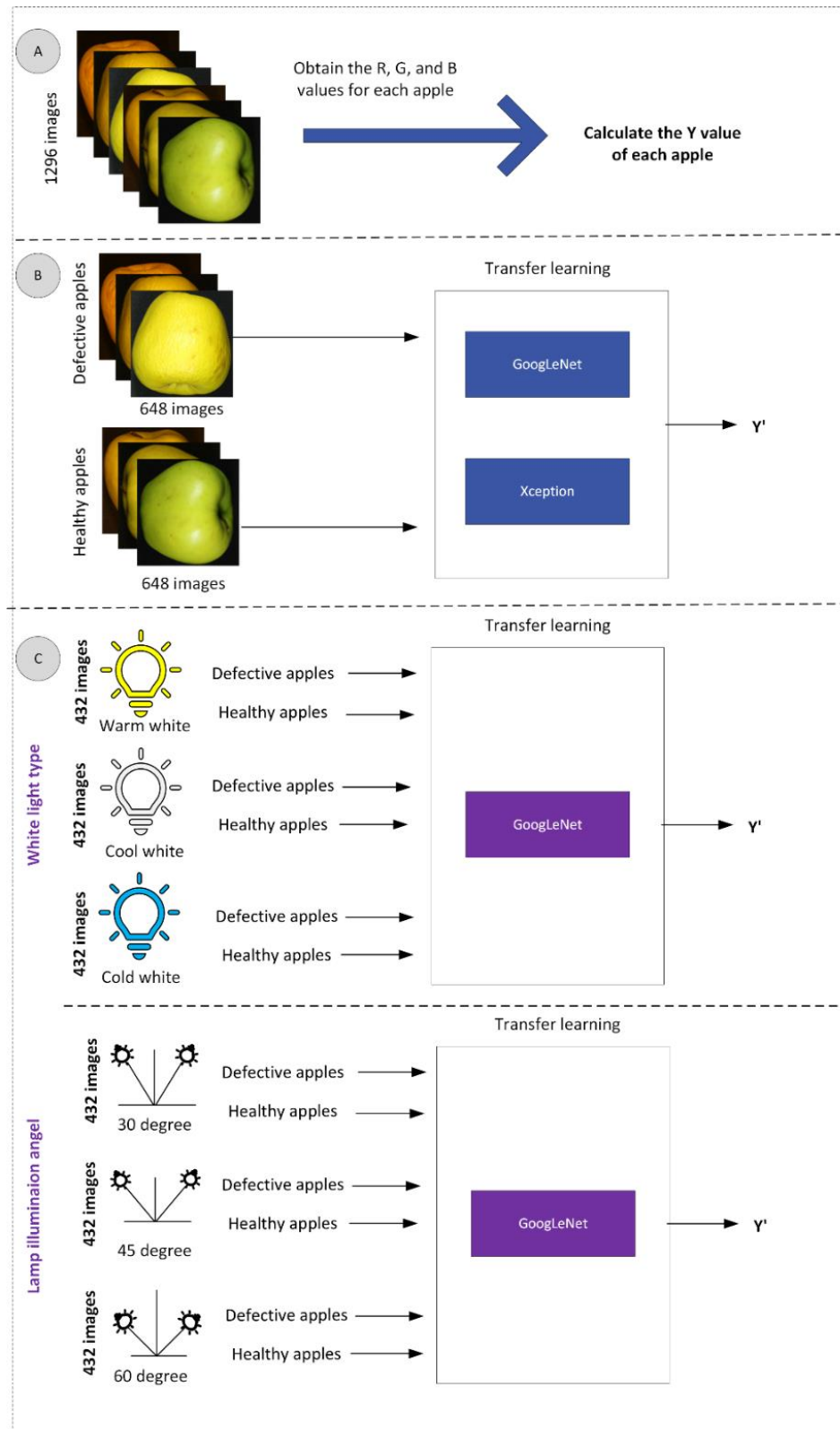


Figure 3. The Proposed Approach, **a.** Calculation of the Y Parameter of All Images **b.** Determination of the Best Parameters of the Models in Estimating the Luminance According to the Defect Types **c.** Estimation of the Luminance According to the Color Temperature and the Lamp Illumination Angle.

The hyperparameters used in the training of the models tested for luminance estimation are listed in Table 3. This study used Stochastic Gradient Descent (SGD) as the optimization method. The momentum value was selected as 0.9, and the learning rates were chosen as 0.001 and 0.0001. The decay value (decrease rate) was determined as 0.00005. Euclidean distance loss was used as the loss function of the models. Batch sizes were tested as 2, 4, 8, 16,

32, 64, and 128. The training period was applied as 50 epochs, and the activation function was determined as ReLU. In this study, GoogLeNet and Xception models were trained using the transfer learning method, and the models' performances were compared. The input dimensions of these models are 224x224x3 and 299x299x3. The images in the dataset were resized to fit the models' input dimensions. One thousand neurons were used in the final layer, and 1 in the last layer of the models, and the prediction performance of both models was evaluated. In addition, the performance of the models was assessed with the 3-fold cross-validation method, and the average values of the criteria for the performance of the models were shared.

To solve the luminance estimation problem, the performance of the models was analyzed using statistical performance measures such as MSE, MAE, RMSE, and MAPE. In addition, luminance estimations were made according to color temperatures and lamp illumination angles using the models and parameters that provided the best estimation results. Since the studies on luminance estimation in literature are limited, a comprehensive analysis was performed in this study by testing different learning rates and batch sizes.

Table 3. Parameters and Values of the Models.

Parameter	Value/Values
Input size	224x224x3 and 299x299x3
Model	GoogLeNet and Xception
Loss function	Euclidean distance loss
Optimizer	SGD
Momentum	0.9
Learning rate	0.001 and 0.0001
Decay	0.00005
Batch size	2, 4, 8, 16, 32, 64, and 128
Epoch	50
Activation function	ReLU

Evaluation Criteria

Electrical criteria

Using the luminous flux and lamp power values of LED lighting sources, electromagnetic radiation amounts and related values such as light efficiency (e), light intensity (I), and average power consumption per illuminance level (APVI) can be calculated (Büyükarıkan, 2022). The formulas for the electrical criteria in this study, which are illuminance level (E), e , I , illuminance level at a point, E_p , and APVI, are given in Equations 2-6.

$$E = \frac{\Phi}{A} \quad (2)$$

$$e = \frac{\Phi}{P} \quad (3)$$

$$I = \frac{\Phi}{2\pi(1 - \cos(\frac{\theta}{2}))} \quad (4)$$

$$E_p = \frac{I \cdot \cos(\theta)}{d^2} \quad (5)$$

$$APVI = \frac{P}{E} \quad (6)$$

Here, Φ is the luminous flux, A is the area of the target scene in square meters, P is the lamp power, I is the light intensity, θ is the lamp position angle value, E_p is the illuminance level of a point p , and d is the hypotenuse distance in meters.

Luminance Criteria

In this study, statistical measures such as MSE (Equation 7), RMSE (Equation 8), MAE (Equation 9), and MAPE (Equation 10) were used to evaluate the luminance estimate. In measures such as MSE, RMSE, and MAE, which measure the differences between the model's estimates and the actual values, the smaller the differences obtained, the more accurate the model's estimates will be. Therefore, the smaller these values indicate that the model performs better. In addition, a MAPE value below 10% indicates that the model's forecasting performance is excellent, and a MAPE value between 10% and 20% indicates that the model's forecasting is successful and reliable (Büyükarıkan, 2022).

$$MSE = \frac{\sum (y_i - \hat{y}_i)^2}{n} \quad (7)$$

$$RMSE = \sqrt{MSE} \quad (8)$$

$$MAE = \frac{\sum |y_i - \hat{y}_i|}{n} \quad (9)$$

$$MAPE = \frac{1}{n} \sum_{i=1}^n \frac{|y_i - \hat{y}_i|}{y_i} * 100 \quad (10)$$

Here, y_i represents the true value, \hat{y}_i represents the predicted value, and n represents the number of samples.

EXPERIMENTAL RESULTS

Lighting Characteristics and Photometric Evaluation

Table 4 lists lamps' photometric and electrical properties with different color temperatures. This study calculated the maximum illuminance level of the surface, APVI, I, and E_p values by considering the angles at which the lamp illuminates the object. In addition, E_p was evaluated at different height values (h value was determined as 30, 35, and 40 cm), and the calculated and measured values are presented in Table 4. The measured E_p values were obtained using a light meter.

Table 4. Evaluation of the Photometric and Electrical Properties of the Lamps.*

Quantity (unit)	Angle (°)	Warm white	Cool white	Cold white
Total luminous flux (lumen)		1612	3000	1300
Total real lamp power (Watt)		17	28	18
e (lumen/Watt)		94.82	107.14	72.22
Maximum illuminance level of the surface (lux)	30	8725.21	16237.98	7036.46
Maximum illuminance level of the surface (lux)	45	7124.10	13258.25	5745.24
Maximum illuminance level of the surface (lux)	60	5037.50	9375.00	4062.50
APVI (Watt/lux)	30	0.0019	0.0017	0.0026
APVI (Watt/lux)	45	0.0024	0.0021	0.0031
APVI (Watt/lux)	60	0.0034	0.0030	0.0044
Calculated I (candela)	30	452.49	842.11	364.91
Calculated I (candela)	45	396.87	738.60	320.06
Calculated I (candela)	60	342.08	636.62	275.87
Average E_p calculated for 30 cm (lux)	30	3978.84	7404.79	3208.74
Average E_p calculated for 30 cm (lux)	45	2849.39	5302.83	2297.89
Average E_p calculated for 30 cm (lux)	60	1736.63	3231.95	1400.51
Average E_p calculated for 35 cm (lux)	30	3040.93	5659.30	2452.36
Average E_p calculated for 35 cm (lux)	45	2177.72	4052.83	1756.22
Average E_p calculated for 35 cm (lux)	60	1327.27	2470.10	1070.38
Average E_p calculated for 40 cm (lux)	30	2376.06	4421.95	1916.18
Average E_p calculated for 40 cm (lux)	45	1701.58	2239.21	1372.24
Average E_p calculated for 40 cm (lux)	60	1037.07	1930.04	836.35
E_p measured for 30 cm (lux)	30	2240	5820	1554
E_p measured for 30 cm (lux)	45	1912	5700	1524
E_p measured for 30 cm (lux)	60	1781	4190	908
E_p measured for 35 cm (lux)	30	1771	4220	1390
E_p measured for 35 cm (lux)	45	1697	3310	960
E_p measured for 35 cm (lux)	60	1189	2710	690
E_p measured for 40 cm (lux)	30	1225	3170	757
E_p measured for 40 cm (lux)	45	951	2510	710
E_p measured for 40 cm (lux)	60	854	2160	475

*The values provided by the manufacturer of the lamps are indicated in bold

The brightness values of the lamps are compared according to their luminous flux or power units; however, since different lamps produce different amounts of light, they are compared with their power units. For this reason, other photometric measures, such as luminous flux, can be used to compare the brightness of different lamps. In addition, when a lamp with a luminous flux of 1000 lumens illuminates an area of 1 square meter, the illuminance level of this

area is calculated as 1000 lux (Auersignal, 2022). Table 5 shows the photometric measurement results of the lamps according to the reference values. In the cabin system, it is assumed that the total luminous flux of the lamps is 1000 lm and that these lamps illuminate a 40x40 cm (0.16 m²) scene.

Table 5. Comparison of the Brightness Values of The Lamps With Reference Values.*

Quantity (unit)	Angle (°)	Warm white	Cool white	Cold white
Total luminous flux (lumen)		1612	3000	1300
Total real lamp power (Watt)		17	28	18
Panel area (m ²)			0.16	
Reference luminous flux (lumen)			1000	
Total lamp power (Watt)		10.55	9.33	13.85
Maximum illuminance level (lux)	30°		5412.66	
Maximum illuminance level (lux)	45°		4419.42	
Maximum illuminance level (lux)	60°		3125.00	

*The values provided by the manufacturer of the lamps are indicated in bold

Luminance Estimation With CNN Models

This study evaluated the GoogLeNet and Xception models used for luminance estimation according to the RMSE criterion (Songwa et al., 2021). These models were compared to the RMSE values obtained from different learning rates and batch sizes. As shown in Table 6, the GoogLeNet model exhibited the best performance, especially at the learning rate of 0.001 and batch size of 8. Under these parameters, RMSE values of 4.139 cd/m² were obtained for defective apples and 3.625 cd/m² for healthy apples. The Xception model generally produced higher RMSE values. This reveals that Xception is not as successful as GoogLeNet in solving this problem. In addition, it is seen that the prediction errors of healthy apples are lower than those of defective apples. This shows that irregularities and faulty structures on the surface negatively affect the prediction performance. Small values in batch size (2, 4, and 8) have achieved better results than large batch sizes (64 and 128). Finally, the GoogLeNet model has shown better performance with small batch sizes and more significant learning rates. These results reveal the elements that show that model selection and hyperparameter optimization should be considered in luminance estimation. In the continuation of this study, the GoogLeNet model was used, and luminance estimation was performed according to color temperatures and lamp illumination angles with a learning rate of 0.001 and a batch size of 8.

Table 6. RMSE Results of Luminance Estimation According to Models (cd/m²).*

Learning rate	Batch size	Xception		GoogLeNet	
		Defective	Healthy	Defective	Healthy
0.001	2	34.363	39.766	6.862	7.113
	4	29.046	29.603	4.580	4.143
	8	31.546	28.425	4.139	3.625
	16	29.441	30.647	8.610	5.343
	32	36.868	30.304	5.471	5.592
	64	40.383	35.295	21.993	58.351
	128	42.447	37.207	98.145	81.800
0.0001	2	44.663	32.322	4.953	6.754
	4	39.849	34.358	4.286	4.428
	8	41.251	35.231	9.323	7.720
	16	42.509	39.191	8.398	5.296
	32	43.932	44.244	9.289	5.871
	64	45.535	48.130	96.937	52.573
	128	85.302	101.339	42.566	70.251

* Best results are shown in bold font

The luminance estimation results performed under different white light types are shown in Table 7. According to the results, RMSE, MSE, MAE, and MAPE values of healthy apples were generally lower than those of defective apples. The lowest RMSE value of 5.023 cd/m² was obtained in cold white light type and healthy apples. In addition, the cold white light type exhibited the best performance with the lowest MSE (3.783), MAE (26.361), and MAPE (11.843%) values compared to other light types. These results show that cold white light provides a more suitable environment for luminance estimation in object illumination. Table 7 shows that station errors are higher in warm and cool white color temperatures.

Table 7. White Light Luminance Estimation (cd/m²) According to Defect Status.*

Color temperature	Defect type	RMSE	MSE	MAE	MAPE (%)
Warm white	Defective	5.150	4.033	27.633	4.549
	Healthy	6.247	5.207	39.103	14.265
Cool white	Defective	6.567	5.958	46.057	15.254
	Healthy	6.027	5.038	38.024	14.729
Cold white	Defective	5.311	3.973	29.668	11.550
	Healthy	5.023	3.783	26.361	11.843

* Best results are shown in bold font

Table 8 shows the effect of the position angle of the illumination source on the luminance estimation. The lowest RMSE value for defective apples was obtained as 5.106 cd/m² at the 60-degree lamp angle, and this angle also provided the lowest MAPE value of 3.909, outperforming other angles. The lowest RMSE value for healthy apples was 6.411 cd/m² at the 45-degree lamp angle. However, defective apples generally obtained lower error values compared to healthy apples. This shows that defective surfaces can increase the prediction accuracy of the models by making the light distribution more apparent. These findings emphasize that the lamp illumination angle is critical in luminance estimation and that the correct angle selection can significantly improve the prediction performance.

Table 8. Lamp Angle Luminance Estimation (cd/m²) According to Defect Conditions.*

Lamp angle (°)	Defect type	RMSE	MSE	MAE	MAPE (%)
30	Defective	7.481	6.329	60.243	15.159
	Healthy	7.546	6.290	65.186	6.876
45	Defective	7.689	6.755	60.599	14.512
	Healthy	6.411	5.500	44.490	6.555
60	Defective	5.106	3.623	26.703	3.909
	Healthy	7.130	5.871	53.278	6.067

* Best results are shown in bold font

Discussion

Color temperature is one factor that changes images' color and luminance properties. Another factor that changes these properties of the image is the angle at which the lamp illuminates the object (Büyükarıkan, 2022). Although different light colors (warm white, cold white, and green light) have been preferred in studies of illumination differences (Buyukarikan and Ulker, 2022; Büyükarıkan and Ülker, 2022; Buyukarikan and Ulker, 2023), the fact that lamp illumination angle on apple is fixed at a 45-degree angle may prevent some surface features from being visible. To best analyze this situation, understanding the effects of different white light color temperatures and lamp illumination angles on image processing and analysis is a critical step in making accurate luminance estimates. This study proposes an application with CNN architecture to estimate the luminance values in the images obtained depending on the color temperature and lamp angle. The study optimizes CNN models with various training parameters and transfer learning. The model that shows the best results with the most appropriate parameters is run, and luminance estimates are made according to the color temperature and lamp illumination angles.

In the literature, studies on image-based luminance estimation are limited. Table 9 shows a comparison of similar studies in the literature. Kayakuş and Çevik (2019) performed luminance estimation with a DNN using R, G, and B pixel values of road images. Yang et al. (2021) recalibrated the illumination settings with the CNN model they proposed in images with different azimuthal angles and color temperatures. Similarly, in this proposed approach, images were obtained using different lamp illumination angles and color temperatures. On the other hand, Songwa et al. (2021) used the Y parameter in their proposed CNN model to estimate luminance from desk images in the office environment. Simon and Uma (2022) used the CNN model to classify texture images using features obtained from different color spaces and the Y parameter. Similarly, this proposed approach's luminance estimation was performed based on the Y parameter using known CNN models. The GoogLeNet model yielded lower RMSE values for the imperfect and perfect apple luminance estimation, with the lowest RMSE of 5.023 cd/m² for color temperature and 5.106 cd/m² for lamp illumination angle. These results show that the GoogLeNet model provides high accuracy in luminance estimation and discriminates defect conditions more effectively.

Table 9. Comparison of Studies in Literature.

Reference	Aim of the study	Dataset/Image count	Method	Best result
Kayakuş and Çevik (2019)	Luminance estimation from road lighting images	100	DNN	MSE: 0.0754
Yang et al. (2021)	Calibration of illumination settings from images	VIDIT: 390	MB-Net	PSNR: 19.3558 and SSIM: 0.7175
Songwa et al. (2021)	Luminance estimation from desk surface images in an office environment	KLED-2020: 1604 and KLED-2019: 4416	LumNet	RMSE: 6.24 cd/m ²
Simon and Uma (2022)	Classification of texture images	DMD: 5640 FMD: 1000	Deep Features (ResNet101) + luminance + SVM	Accuracy: 73.63
This study	Estimation of luminance from images based on color temperature and lamp illumination angle	1296	GoogLeNet	Color temperature RMSE: 5.023 cd/m ² Lamp illumination angle RMSE: 5.106 cd/m ²

Advantages and Limitations of the Study

There are several advantages of this study. First, the luminance estimations made using CNN models show high accuracy, especially with low RMSE values obtained with the GoogLeNet model. Considering the effects of color temperature and lamp illumination angle allows the model to work effectively under different lighting conditions. Using the CNN-based approach in this study contributes to obtaining more accurate estimations by enabling the model to focus more on essential features in the visual data. In the luminance estimations made between defective and healthy cases, the fact that the model effectively distinguishes the differences provides an excellent advantage for real-world applications.

There are also some limitations to this study. The limited number of samples in the dataset may limit the model's generalization ability, and larger datasets may be required. The datasets used were limited to certain lighting conditions and camera types, which may limit the generalizability of the results under different conditions. Creating the datasets with a single camera may reveal the problem of device dependency. The results obtained using different camera types may be inconsistent with the existing findings. In addition, lighting conditions also have a significant effect. The model is not guaranteed to work with the same success in every lighting condition. Moreover, the impact of the lamp angle on the luminance estimation may become more complex and require more parameters for the model's accuracy, limiting its applicability in practice. In addition, images taken under controlled lighting conditions may not accurately reflect changing lighting conditions. Therefore, to increase the flexibility of the model, its evaluation under natural and different lighting scenarios will allow a better understanding of real-time applications.

CONCLUSION AND RECOMMENDATIONS

This study used a dataset containing color temperatures and lamp illumination angles to estimate image-based luminance. Well-known CNN models, GoogLeNet and Xception model were used to perform luminance estimation of defective and healthy apples with different training parameters. The best RMSE value was obtained with the GoogLeNet model with a learning rate of 0.001 and a batch size of 8. According to color temperatures, the lowest RMSE value for defective apples was found in warm white light, and healthy apples in cold white light. The best luminance estimation RMSE value obtained under cold white light was 5.023 cd/m². According to the illumination source position angle, the lowest RMSE value was observed at 60 degrees for defective and 45 degrees for healthy apples. The article demonstrates that deep learning architectures can be used in luminance estimation and the usefulness of one of these architectures, the GoogLeNet model.

In future studies, more extensive and more diverse datasets can be used to improve the performance of illumination and luminance estimation. Moreover, the prediction accuracy of CNN-based algorithms can be further enhanced by increasing the diversity of different camera types and datasets to reduce device dependency. In addition, testing CNN-based models under natural and various lighting conditions can provide a better understanding of different scenarios that may be encountered in real-time applications and optimize model performance. Therefore, a comprehensive analysis can be performed using sensors for real-time applications.

ACKNOWLEDGEMENT

This work was supported by the Scientific Research Project at Konya Technical University, Konya, Turkey (No. 201113006). This study is part of the doctoral thesis of Büyükarıkan (2022), which was conducted under the supervision of Prof. Dr. Erkan Ülker.

Artificial Intelligence Contribution Statement

This manuscript was entirely written, edited, analyzed, and prepared without the assistance of any artificial intelligence tools. All content, including text, data analysis, and figures, was solely generated by the authors.

REFERENCES

- Aleixos, N., Blasco, J., Navarron, F., & Moltó, E. (2002). Multispectral inspection of citrus in real-time using machine vision and digital signal processors. *Computers and electronics in agriculture*, 33 (2), 121-137. [https://doi.org/10.1016/S0168-1699\(02\)00002-9](https://doi.org/10.1016/S0168-1699(02)00002-9)
- Auersignal. All about luminous intensity, luminous flux & illuminance. (2022). <https://www.auersignal.com/en/technical-information/visual-signallingequipment/luminous-intensity/#What%20is%20the%20solid%20angle?> Accessed 23.7.2022
- Benweilight. Aydınlatma ışını açılarının yorumlanması ve analizi. (2021). <https://tr.benweilight.com/info/interpretation-and-analysis-of-illumination-be-61992668.html> Accessed 21.12.2024.
- Brosnan, T. & Sun, D.-W. (2004). Improving quality inspection of food products by computer vision—a review. *Journal of food engineering*, 61 (1), 3-16. [https://doi.org/10.1016/S0260-8774\(03\)00183-3](https://doi.org/10.1016/S0260-8774(03)00183-3)
- Buyukarikan, B. & Ulker, E. (2022). Classification of physiological disorders in apples fruit using a hybrid model based on convolutional neural network and machine learning methods. *Neural Computing and Applications*, 34 (19), 16973-16988. <https://doi.org/10.1007/s00521-022-07350-x>
- Buyukarikan, B. & Ulker, E. (2023). Classification of physiological disorders in apples using deep convolutional neural network under different lighting conditions. *Multimedia Tools and Applications*, 82 (21), 32463-32483. <https://doi.org/10.1007/s11042-023-14766-7>
- Büyükarıkan, B. (2022). Aydınlatmanın görüntü işleme problemlerine etkisinin yapay zeka teknikleri kullanılarak analizi. Doktora Tezi. Konya Teknik Üniversitesi Lisansüstü Eğitim Enstitüsü Bilgisayar Mühendisliği Anabilim Dalı, Konya 147s.
- Büyükarıkan, B. & Ülker, E. (2022). Using convolutional neural network models illumination estimation according to light colors. *Optik*, 271, 170058. <https://doi.org/10.1016/j.ijleo.2022.170058>
- Catalbas, M. C. & Kobav, M. B. (2022). Measurement of correlated color temperature from RGB images by deep regression model. *Measurement*, 195, 111053. <https://doi.org/10.1016/j.measurement.2022.111053>
- Chollet, F. (2017). Xception: Deep learning with depthwise separable convolutions. *Proceedings of the IEEE conference on computer vision and pattern recognition (CVPR) 2017* (pp. 1251-1258). IEEE.
- Girolami, A., Napolitano, F., Faraone, D. & Braghieri, A. (2013). Measurement of meat color using a computer vision system. *Meat science*, 93 (1), 111-118. <https://doi.org/10.1016/j.meatsci.2012.08.010>
- Holtzschue, L. (2012). *Understanding color: an introduction for designers*. John Wiley & Sons.
- Hong, S., Kim, I., Kim, H., Sohn, A., Choi, A. S., Sung, M. & Jeong, J. W. (2017). Evaluation of the visibility of colored objects under LED lighting with various correlated color temperatures. *Color Research & Application*, 42 (1), 78-88. <https://doi.org/10.1002/col.22048>
- Huang, Y.-S., Luo, W.-C., Wang, H.-C., Feng, S.-W., Kuo, C.-T. & Lu, C.-M. (2017). How smart LEDs lighting benefit color temperature and luminosity transformation. *Energies*, 10 (4), 518. <https://doi.org/10.3390/en10040518>

- Huang, Z. & Wei, M. (2021). Effects of adapting luminance and CCT on appearance of white and degree of chromatic adaptation, part II: extremely high adapting luminance. *Optics Express*, 29 (25), 42319-42330. <https://doi.org/10.1364/OE.27.009276>
- Iacomussi, P., Radis, M., Rossi, G. & Rossi, L. (2015). Visual comfort with LED lighting. *Energy Procedia*, 78, 729-734. <https://doi.org/10.1016/j.egypro.2015.11.082>
- Ileri, D., Belal, E., Okinda, C., Makange, N. & Ji, C. (2019). A computer vision system for defect discrimination and grading in tomatoes using machine learning and image processing. *Artificial Intelligence in Agriculture*, 2, 28-37. <https://doi.org/10.1016/j.aiia.2019.06.001>
- Kamath, V., Kurian, C. P. & Padiyar, U. S. (2022). Development of bayesian neural network model to predict the correlated color temperature using digital camera and Macbeth ColorChecker chart. *IEEE Access*, 10, 55499-55507. <https://doi.org/10.1109/ACCESS.2022.3177195>
- Kandpal, L. M., Lee, J., Bae, J., Lohumi, S. & Cho, B.-K. (2019). Development of a low-cost multi-waveband LED illumination imaging technique for rapid evaluation of fresh meat quality. *Applied Sciences*, 9 (5), 912. <https://doi.org/10.3390/app9050912>
- Kayakuş, M. & Çevik, K. K. (2019). Estimating luminance measurements in road lighting by deep learning method. *Artificial Intelligence and Applied Mathematics in Engineering Problems: Proceedings of the International Conference on Artificial Intelligence and Applied Mathematics in Engineering (ICAIAME 2019)* (pp. 940-948).
- Kim, J. H., Jang, J. W. & Jang, K. J. (2018). A color adjustment convolutional neural network for image superresolution. *2018 International Conference on Electronics, Information, and Communication (ICEIC)* (pp. 1-2).
- Kocabey, S. (2008). İç hacimlerde aydınlık düzeyi dağılımının bulunması ve sonlu elemanlar yöntemi ile incelenmesi. Doktora Tezi. Marmara Üniversitesi Fen Bilimleri Enstitüsü Elektrik Eğitimi Anabilim Dalı, İstanbul 155s.
- Li, J., Chen, L., Huang, W., Wang, Q., Zhang, B., Tian, X., Fan, S. & Li, B. (2016). Multispectral detection of skin defects of bi-colored peaches based on vis-NIR hyperspectral imaging. *Postharvest Biology and Technology*, 112, 121-133. <https://doi.org/10.1016/j.postharvbio.2015.10.007>
- Liu, Q., Huang, Z., Li, Z., Pointer, M. R., Zhang, G., Liu, Z., Gong, H. & Hou, Z. (2020a). A field study of the impact of indoor lighting on visual perception and cognitive performance in classroom. *Applied Sciences*, 10 (21), 7436. <https://doi.org/10.3390/app10217436>
- Liu, Y., Colburn, A. & Inanici, M. (2020b). Deep neural network approach for annual luminance simulations. *Journal of Building Performance Simulation*, 13 (5), 532-554. <https://doi.org/10.1080/19401493.2020.1803404>
- Luo, M. R. (2011). The quality of light sources. *Coloration Technology*, 127 (2), 75-87. <https://doi.org/10.1111/j.1478-4408.2011.00282.x>
- Ma, L., Sun, K., Tu, K., Pan, L. & Zhang, W. (2017). Identification of double-yolked duck egg using computer vision. *PloS one*, 12 (12), e0190054. <https://doi.org/10.1371/journal.pone.0190054>
- Manav, B. (2005). Ofislerde aydınlık düzeyi, parlıltı farkı ve renk sıcaklığının görsel konfor koşullarına etkisi: Bir model çalışması. Doktora Tezi. İstanbul Teknik Üniversitesi Fen Bilimleri Enstitüsü Mimarlık Anabilim Dalı, İstanbul 147s.
- Nie, T. & Lv, X. (2023). Deep Learning-Based Machine Color Emotion Generation. *International Journal of Mobile Computing and Multimedia Communications (IJMCMC)*, 14 (1), 1-14.
- Odabas, M. S., Şenyer, N. & Kurt, D. (2023). Determination of quality grade of tobacco leaf by image processing on correlated color temperature. *Concurrency and Computation: Practice and Experience*, 35 (2), e7506. <https://doi.org/10.1002/cpe.7506>

Özkaya, M. & Tüfekçi, T. (2011). Aydınlatma tekniği. Birsen Yayınevi.

Saldaña, E., Siche, R., Luján, M. & Quevedo, R. (2013). Computer vision applied to the inspection and quality control of fruits and vegetables. *Brazilian journal of food technology*, 16, 254-272. <https://doi.org/10.1590/S1981-67232013005000031>

Sharma, G. & Bala, R. (2017). *Digital color imaging handbook*. CRC press.

Shi, B. & Chen, Z. (2021). A layer-wise multi-defect detection system for powder bed monitoring: Lighting strategy for imaging, adaptive segmentation and classification. *Materials & Design*, 210, 110035. <https://doi.org/10.1016/j.matdes.2021.110035>

Simon, A. P. & Uma, B. (2022). DeepLumina: A method based on deep features and luminance information for color texture classification. *Computational Intelligence and Neuroscience*, 2022 (1), 9510987. <https://doi.org/10.1155/2022/9510987>

Sims, P., Lai, Y.-Y. & Jory, T. (2021). A Review of Various Models for Classifying Light Source Color Rendition and Guide to Using LEDs to Achieve Fidelity Color Rendering for Retail and Other Indoor Environments, https://www.luminus.com/datasheets/WhitePaper_Rev1_Color_Rendering_211130.pdf Accessed 21.06.2022.

Smith, N. (2000). *Lighting for Health and Safety* (Vol. 1). Butterworth Heinemann Oxford.

Songwa, P. U., Saeed, A., Bhardwaj, S., Kruisselbrink, T. W. & Ozcelebi, T. (2021). LumNet: Learning to Estimate Vertical Visual Field Luminance for Adaptive Lighting Control. *Proceedings of the ACM on Interactive, Mobile, Wearable and Ubiquitous Technologies*, 5 (2), 1-20. <https://doi.org/10.1145/3463500>

Sumon, M. B. U. (2022), *Deep Learning Methods for Classification of Photometric Images of Materials*. Master Thesis. Norwegian University of Science and Technology 77p.

Szegedy, C., Liu, W., Jia, Y., Sermanet, P., Reed, S., Anguelov, D., Erhan, D., Vanhoucke, V. & Rabinovich, A. (2014). Going deeper with convolutions. *Proceedings of the IEEE conference on computer vision and pattern recognition* (pp. 1-9).

Unay, D. & Gosselin, B. (2005). Artificial neural network-based segmentation and apple grading by machine vision. *IEEE International Conference on Image Processing 2005* (pp. II-630).

Wang, Z., Dong, Y., Sui, X., Shao, X., Li, K., Zhang, H., Xu, Z. & Zhang, D. (2024). An artificial intelligence-assisted microfluidic colorimetric wearable sensor system for monitoring of key tear biomarkers. *npj Flexible Electronics*, 8 (1), 35. <https://doi.org/10.1038/s41528-024-00321-3>

Wu, Y.-h., Hu, Y.-h., Jiang, F. & Zhang, L.-h. (2010). Design of temperature measurement system based on two-color imaging in adaptive optics of CCD. *5th International Symposium on Advanced Optical Manufacturing and Testing Technologies: Optical Test and Measurement Technology and Equipment*, 1062-1067. <https://doi.org/10.1117/12.865571>

Xu, P., Tan, Q., Zhang, Y., Zha, X., Yang, S. & Yang, R. (2022). Research on maize seed classification and recognition based on machine vision and deep learning. *Agriculture*, 12 (2), 232. <https://doi.org/10.3390/agriculture12020232>

Yang, H.-H., Chen, W.-T., Luo, H.-L. & Kuo, S.-Y. (2021). Multi-modal bifurcated network for depth guided image relighting. *Proceedings of the IEEE/CVF Conference on Computer Vision and Pattern Recognition* (pp. 260-267).

Yang, Q. (1994). An approach to apple surface feature detection by machine vision. *Computers and electronics in agriculture*, 11 (2-3), 249-264. [https://doi.org/10.1016/0168-1699\(94\)90012-4](https://doi.org/10.1016/0168-1699(94)90012-4)